Sustained expression of PGC-1α in the rat nigrostriatal system selectively impairs dopaminergic function

C. Ciron, S. Lengacher, J. Dusonchet, P. Aebischer and B.L. Schneider*

Brain Mind Institute, Ecole Polytechnique Fédérale de Lausanne (EPFL), Lausanne, Switzerland

Mitochondrial dysfunction and oxidative stress have been implicated in the etiology of Parkinson's disease. Therefore, pathways controlling mitochondrial activity rapidly emerge as potential therapeutic targets. Here, we explore the neuronal response to prolonged overexpression of peroxisome proliferator-activated receptor gamma coactivator-1 alpha (PGC-1α), a transcriptional regulator of mitochondrial function, both *in vitro* and *in vivo*. In neuronal primary cultures from the ventral midbrain, PGC-1α induces mitochondrial biogenesis and increases basal respiration. Over time, we observe an increasing proportion of the oxygen consumed by neurons which are dedicated to adenosine triphosphate production. In parallel to enhanced oxidative phosphorylation, PGC-1α progressively leads to a decrease in mitochondrial polarization. In the adult rat nigrostriatal system, adeno-associated virus (AAV)-mediated overexpression of PGC-1α induces the selective loss of dopaminergic markers and increases dopamine (DA) catabolism, leading to a reduction in striatal DA content. In addition, PGC-1α prevents the labeling of nigral neurons following striatal injection of the fluorogold retrograde tracer. When PGC-1α is expressed at higher levels following intranigral AAV injection, it leads to overt degeneration of dopaminergic neurons. Finally, PGC-1α overexpression does not prevent nigrostriatal degeneration in pathologic conditions induced by α-synuclein overexpression. Overall, we find that lasting overexpression of PGC-1α leads to major alterations in the metabolic activity of neuronal cells which dramatically impair dopaminergic function *in vivo*. These results highlight the central role of PGC-1α in the function and survival of dopaminergic neurons and the critical need for maintaining physiological levels of PGC-1α activity.

INTRODUCTION

Mitochondrial dysfunction is a crucial factor in the pathogenesis of neurodegenerative disorders affecting the aging brain ([1]). In addition to energy supply, mitochondria integrate extracellular signals and carry out essential cellular functions determining neuronal survival and death. Maintaining a pool of healthy mitochondria and eliminating dysfunctional mitochondria appear crucial for cellular homeostasis. Indeed, perturbations in mitochondrial energy metabolism lead to reduced adenosine triphosphate (ATP) levels, impaired calcium buffering and increased production of reactive oxygen species (ROS) ([2]), potential contributors to neuronal degeneration.

In the broad array of environmental and genetic factors that underlie the etiology of Parkinson's disease (PD),

mitochondrial dysfunction emerges as a common denominator. PD-related toxins, such as 1-methyl-4-phenyl-1,2,3,6-tetra-hydropyridine (MPTP) and rotenone, which provoke selective degeneration of nigral dopaminergic neurons, both inhibit the respiratory chain complex I ([3]). Furthermore, some evidence for reduced complex I activity in PD brain tissue highlights impairments in the electron transport chain (ETC) as a possible cause of neurodegeneration.

The association of several genes with familial and sporadic forms of PD has brought additional evidence regarding the link between mitochondrial dysfunction and the pathogenic process leading to PD ([4]). Alpha-synuclein (αSyn), parkin, PTEN-induced putative kinase 1 (PINK1), DJ-1 and leucine-rich repeat kinase 2 have been found to affect mitochondrial function. In particular, PINK1 and parkin play critical roles

*To whom correspondence should be addressed at: AI 2241 Station 19, Lausanne 1015, Switzerland. Tel: +41 216939505; Fax: +41 216939520; Email: bernard.schneider@epfl.ch

in the quality control of mitochondria (5–7). The αSyn protein, which is considered central to PD pathogenesis, can directly interact with the mitochondria (8–10). Both cellular and animal models demonstrate that αSyn can affect ETC components and thereby lead to the excessive production of ROS in dopaminergic neurons (8). Mutations or elevated levels of αSyn accelerate the formation of protofibrils or oligomers, which may form pores in biological membranes and increase mitochondrial permeability in neurons (11).

Therefore, pathways controlling mitochondrial function rapidly emerge as potential therapeutic targets. In this context, the transcriptional coactivator peroxisome proliferator-activated receptor gamma (PPARγ) coactivator-1 alpha (PGC-1α) is considered a master regulator of mitochondrial biogenesis and metabolism (12,13). In cooperation with estrogen-related receptor alpha (ERRα), NRF1 and NRF2, PGC-1α controls oxidative phosphorylation through expression of genes involved in the mitochondrial respiratory chain (14,15). In parallel, PGC-1α promotes the expression of enzymes important for the detoxification of ROS (16).

Recent publications have highlighted perturbations of PGC-1α activity in neurodegenerative disorders, with a down-regulation of PGC-1α or its major target genes in Huntington's disease (HD) (17,18), Alzheimer's patients (19) and PD (20,21). In addition, genetic variations in the *PGC-1α* gene delay the onset of motor symptoms in HD by several years (22). PGC-1α shows neuroprotective effects in a rodent model of HD (18). Two recent studies demonstrate that PGC-1α transgenic expression improves the survival and function of motor neurons in the SOD1^{G93A} mouse model of amyotrophic lateral sclerosis (23,24). In this encouraging context, PGC-1α has appeared as a promising therapeutic target in PD, at the intersection between mitochondrial dysfunction and resistance to oxidative stress.

Here, we have evaluated the effect of PGC-1α expression in the dopaminergic system to assess how this regulator of mitochondrial function may control neuronal function and survival. PGC-1α overexpression using recombinant adeno-associated virus (rAAV) leads to profound alterations in neuronal metabolic profile, consistent with changes in mitochondrial biogenesis, ATP production, mitochondrial polarization and expression of genes implicated in mitochondrial function. In the adult rat nigrostriatal system, PGC-1α induces dose-dependent effects, ranging from a selective loss of dopaminergic markers to overt degeneration of nigral neurons, consistent with a reduction in striatal DA. These results demonstrate that nigral dopaminergic are critically sensitive to the modifications in mitochondrial homeostasis induced by PGC-1α. To explore the interaction between PGC-1α and pathological conditions related to PD, we further investigate the effect of PGC-1α in neurons expressing human αSyn.

RESULTS

PGC-1α induces mitochondrial biogenesis and increases respiration rates in neurons from the ventral midbrain

In order to assess the effect of PGC-1α expression on the mitochondrial function of neuronal cells *in vitro*, we used primary neuronal cultures derived from the mouse ventral midbrain.

These cultures were purely neuronal and contained a small fraction of neurons expressing the dopaminergic markers tyrosine hydroxylase (TH) and DAT. Seven-day-old neuronal cultures were infected with an identical dose of the AAV2/6-PGC-1α or AAV2/6-GFP vectors. To fluorescently label mitochondria, neurons were re-infected 3 days later with an AAV2/6 vector encoding the red fluorescent protein fused to a mitochondrial localization signal (MitoDsRed). Neurons were analyzed 4 days later by flow cytometry (Fig. 1). Neurons expressing PGC-1α and MitoDsRed showed a more than 5-fold increase in the mean Cy5 fluorescence intensity (306.9 ± 93.0) when compared with the control groups expressing GFP/MitoDsRed or MitoDsRed only (56.2 ± 9 and 53.7 ± 0.9, respectively), reflecting massive mitochondrial biogenesis in response to PGC-1α expression.

To further investigate the role of PGC-1α in cellular bioenergetics, the oxygen consumption of cultured midbrain neurons was measured using the XF-24 Analyzer (Fig. 2A–D). Seven-day-old cultures were infected with AAV2/6-PGC-1α or with a non-coding vector as control. Real-time measurements of oxygen consumption rate (OCR) were made at days 5 (Fig. 2A and B) and 7 post-infection (Fig. 2C and D). At 5 days post-infection, neurons overexpressing PGC-1α showed a clear increase in the basal OCR, which remained significantly higher until day 7. To further decipher the neuronal response to PGC-1α, we applied oligomycin to inhibit ATP synthase activity, and FCCP, a mitochondrial protonophore uncoupling oxidative phosphorylation and dissipating the mitochondrial membrane potential. The difference between untreated and oligomycin-treated cells defines the OCR dedicated to ATP production. Following FCCP exposure, the OCR reflects maximal respiration, and the difference between this level and the basal rate represents the reserve respiration capacity. By measuring these parameters at 5 and 7 days post-infection, we observed a shift in the effect of PGC-1α (Fig. 2B and D). Between day 5 and day 7, OCR corresponding to ATP production increased in response to PGC-1α, and appeared significantly increased only at day 7. Conversely, maximal respiration rate in the presence of FCCP, which reflects the capacity of the cells to respond to high ATP demand, was significantly increased at day 5 and no more different at day 7. Similarly, the spared respiratory capacity was significantly increased only at day 5.

Altogether, these data suggest that the increase in OCR at the basal level initially reflects the increase in the mitochondrial mass coupled with oxidative phosphorylation. With time in culture, neurons continue to consume more oxygen, which is increasingly utilized for ATP production. However, neuronal capacity to elevate its metabolic rate and accommodate rapid increases in metabolic demand is no more different from control condition. Therefore, it appears that neurons tend to maximize basal ATP production in response to PGC-1α.

PGC-1α induces changes in the expression of genes related to mitochondrial function and polarization

To further investigate how PGC-1α could impact on mitochondrial function in mesencephalic neuronal cultures over time, we measured changes in the expression of 84 mitochondrial genes. Seven-day-old midbrain cultures infected with
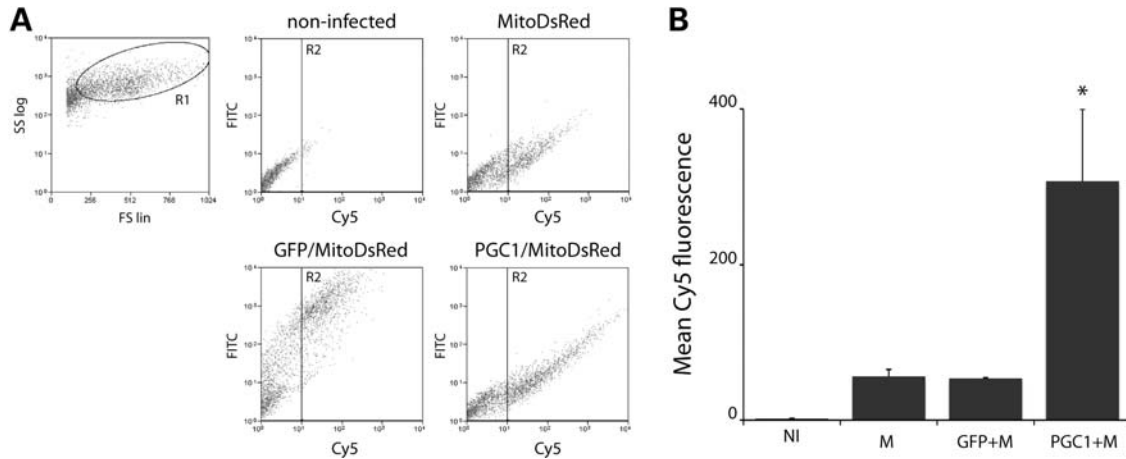
Figure 1. Mitochondrial biogenesis in neurons over-expressing PGC-1α. Primary neuronal culture from mouse ventral midbrain was cultured for 7 days and then transduced with AAV2/6 encoding either PGC1 or GFP. Three days later, the neurons were infected with a vector encoding the MitoDsRed fluorescent protein and analyzed by flow cytometry. Control conditions include non-infected (NI) neurons and neurons infected with the MitoDsRed (M) vector only. (**A**) Representative flow cytometry dot plots: living cells were gated in region R1 of the FS/SS plot. Average Cy5 fluorescence intensity was determined for each group on cells gated in region R2, identified as the population of neurons expressing the MitoDsRed fluorescent protein. (**B**) PGC1 neurons show a clear increase in Cy5 fluorescence reflecting mitochondrial biogenesis. One-way ANOVA with Newman–Keuls *post hoc* test: NI, $n = 2$; M, $n = 2$; GFP, $n = 3$; PGC1, $n = 3$; *$P < 0.05$.
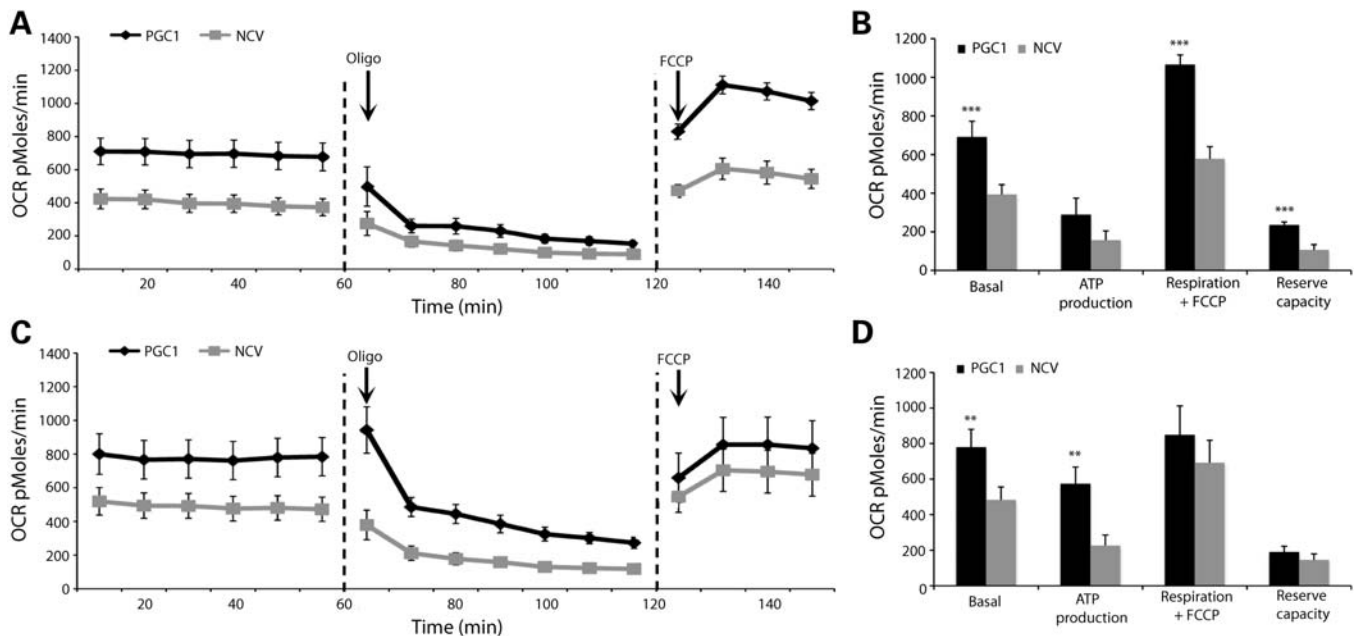

Figure 2. Cellular respiration in neurons over-expressing PGC-1α. (**A–D**) Primary neuronal cultures were infected with either the NCV or the PGC1 vector at day 7. Analysis of cellular respiration was performed at 5 (A) and 7 (C) days post-infection. OCRs were measured on 10 wells per group in basal conditions during 60 min. In each group, a subset of four wells was then treated with 5 μM oligomycin (ATP synthase inhibitor) and OCR was measured during 60 min. Finally, another subset of five wells per group was exposed to 20 μM FCCP (mitochondrial protonophore) and the OCR was measured during 30 min. (B and D) Based on these measurements, we assessed the following OCRs: basal ($n = 10$), dedicated to ATP production ($n = 4$), in presence of FCCP ($n = 5$) and reserve capacity ($n = 5$). Student's *t*-test: **$P < 0.01$, ***$P < 0.001$.

either AAV2/6-PGC-1α or a non-coding vector were analyzed at 5 (Fig. 3A) and 7 days (Fig. 3B) post-infection. The real-time PCR array includes nuclear genes related to various mitochondrial functions, such as the intrinsic apoptotic pathway or molecular transport across inner and outer membranes, which controls the transfer of metabolites for the ETC and oxidative phosphorylation as well as ions implicated in mitochondrial

membrane polarization. Several genes are also implicated in mitochondrial fusion, fission and localization.

At 5 days post-infection (Fig. 3A), we observed several significant changes in gene expression that may impact mitochondrial polarization. *BCL2/adenovirus E1B interacting protein 3* (Bnip3) and *ADP/ATP translocase* (Slc25a4), two genes that can promote proton leakage, were 3- and 1.5-fold
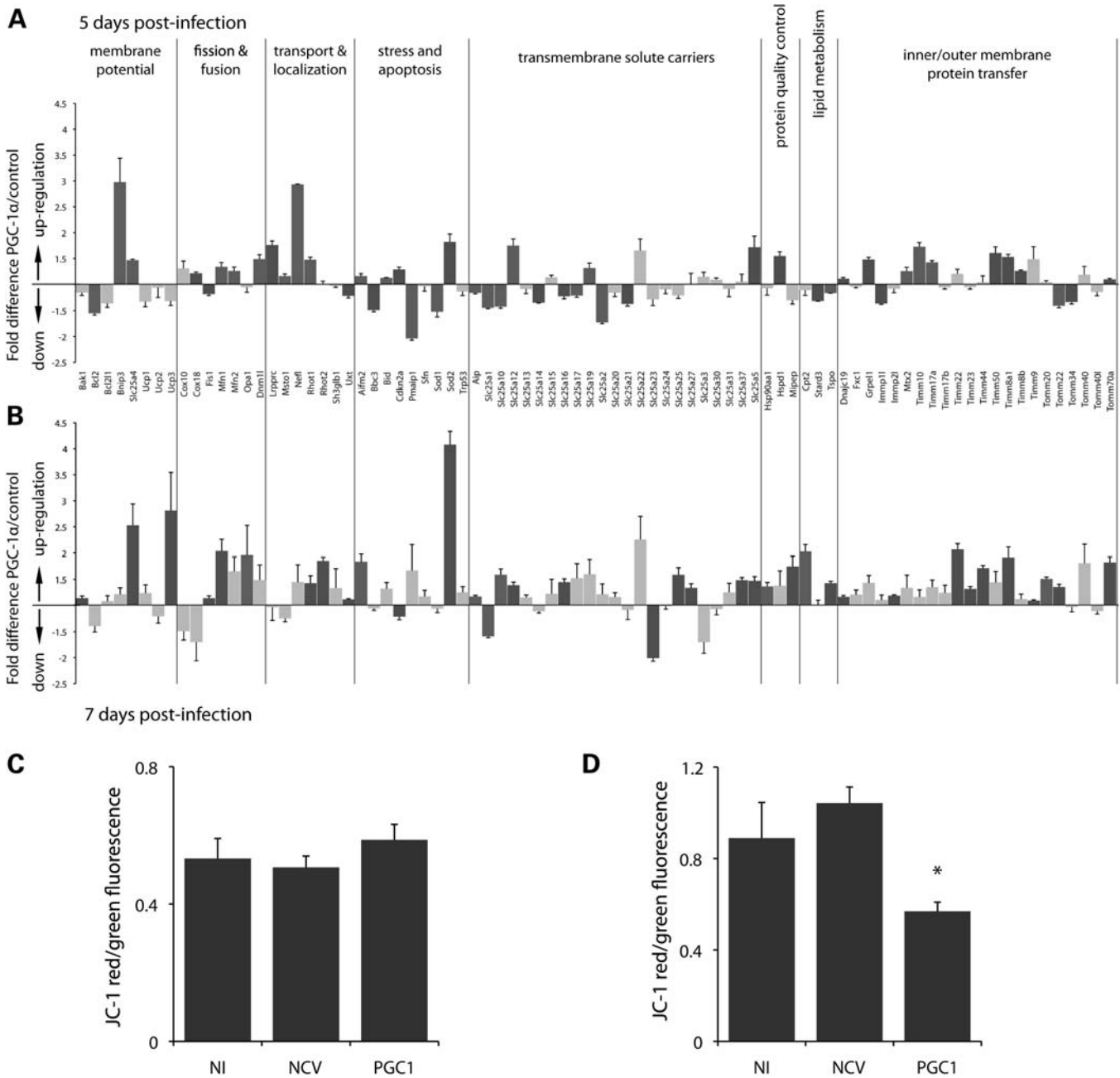
Figure 3. Mitochondrial transcriptome analysis of neuronal cultures overexpressing PGC-1α. Seven-day-old primary neuronal cultures from mouse ventral midbrain were infected with either a NCV or a vector encoding PGC-1α (PGC1). PCR arrays were performed at days 5 (**A**) and 7 (**B**) post-infection, to measure changes in the expression of 84 nuclear genes involved in various mitochondrial functions. Dark grey columns indicate significant changes in gene expression ($n = 4$, Student's t-test, $P < 0.05$). (**C** and **D**) To analyze mitochondrial membrane potential, neurons were incubated with the JC-1 sensor at 5 (C) and 8 (D) days post-infection and the ratio green/red fluorescence measured. One-way ANOVA with Newman–Keuls *post hoc* test: NI, $n = 7$; NCV, $n = 8$; PGC1, $n = 7$; *$P < 0.05$.

up-regulated, respectively. We also measured a 1.6-fold down-regulation of *Bcl2*, which maintains mitochondrial potential by regulating proton flux (25).

PGC-1α also induced expression of genes implicated in mitochondrial fusion, with a 1.3-fold up-regulation of both *mitofusin 1* (Mfn1) and *mitofusin 2* (Mfn2), and a significant 1.2-fold down-regulation of the *mitochondrial fission*

protein 1 (Fis1). At day 5, we further noticed an up-regulation of most genes implicated in mitochondrial transport and localization, such as the *neurofilament light polypeptide* (Nefl) and *MIRO-1* (Rhot1).

At 7 days post-infection (Fig. 3B), the number of genes with significant changes in expression further increased. In particular, we noticed again a 2.5-fold up-regulation of the *ADP/ATP*

translocase (Slc25a4). The *Mfn1* and *Opa1* genes involved in mitochondrial fusion were also up-regulated. We measured an important 4.1-fold up-regulation of the antioxidant gene *Sod2* and an overall increase in the expression of transmembrane solute carriers and proteins implicated in the transfer of proteins across inner/outer mitochondrial membranes.

PGC-1α overexpression induces mitochondrial depolarization

The observed metabolic response to PGC-1α and the pattern of gene expression changes are indicative of potential effects of PGC-1α on mitochondrial membrane potential in mesencephalic neurons. Therefore, we further analyzed mitochondrial membrane potential using the JC-1 sensor at 5 and 8 days post-infection (Fig. 3C and D, respectively). When JC-1 enters the mitochondria, it reversibly forms J-aggregates and thereby produces red fluorescence as a function of the mitochondrial membrane potential. Consequently, mitochondrial depolarization is indicated by a decrease in the red/green fluorescence intensity ratio. At 5 days, no significant differences were observed between groups. However, at 8 days post-infection, ventral midbrain neurons expressing PGC-1α showed a significant decrease in the red/green fluorescence intensity ratio, when compared with neurons either non-infected or infected with a non-coding control vector. This result indicates that constant expression of PGC-1α indeed leads to significant mitochondrial membrane depolarization in ventral midbrain neurons. However, as we observed gene expression and metabolic changes evolving over time in culture, it is important to determine their long-term effect *in vivo*. In addition, primary cultures of ventral midbrain neurons contain mixed populations of neurons with only a fraction of dopaminergic neurons. Therefore, it is important to further address what are the consequences of PGC-1α overexpression specifically on the population of nigral dopaminergic neurons.

Recombinant AAV-mediated overexpression of PGC-1α in the nigrostriatal system of adult rats

We sought to explore the effect of PGC-1α expression on dopaminergic neurons *in vivo*, following unilateral injections of AAV2/6 vectors. We used two modes of administration, based on the ability of AAV2/6 vectors to transduce nigral neurons either via direct injection at the level of the substantia nigra *pars compacta* (SNpc) or by retrograde transport of the vector from nerve terminals following intrastriatal injection. These routes of administration differ by the pattern of transduction obtained. Direct intranigral injection leads to robust transgene expression mainly in the SNpc with a minimal viral dose (5×10^6 TUs) (PGC1 Hi). The intrastriatal injection of 6×10^7 TUs transduces striatal neurons as well as the distant nigral neurons by retrograde transport of the viral particles along axonal projections. This mode of vector injection leads to a lower level of transgene expression in nigral dopaminergic neurons when compared with direct intranigral injections, and will therefore be referred as 'PGC1 Lo'. A similar intrastriatal injection of an AAV2/6 vector expressing GFP demonstrated retrograde transduction of $55.7 \pm 9.9\%$ of the nigral neurons expressing the dopaminergic marker TH.

Both modes of injection led to a robust expression of PGC-1α at 3 months post-injection, as demonstrated by immunostainings (Fig. 4A and B). To quantify the level of PGC-1α mRNA expression induced, we performed a reverse transcription-quantitative PCR (RT–qPCR) on striatal and SNpc samples from PGC1 Hi and PGC1 Lo rats sacrificed at 3 weeks post-injection (Table 1). Following nigral injection, we measured a 399.5 ± 182.2-fold increase in the abundance of the PGC-1α transcript in the SNpc, when compared with the endogenous level in the non-injected control side. Expectedly, there was no difference in striatal PGC-1α expression. In contrast, rats injected in the striatum showed a modest increase in PGC-1α expression in the SNpc, with a 4.5 ± 0.5-fold difference when compared with non-injected side. In the injected striatum, the overall increase appeared of similar amplitude (4.0 ± 1.0-fold). However, striatal vector deposits result in local expression of exogenous PGC-1α, which adds to the high level of endogenous PGC-1α typically observed in striatal tissue (26). Therefore, one should consider the dilution effect of measuring the localized expression of exogenous PGC-1α as part of the large striatal structure.

Overexpression of PGC-1α induced mitochondrial biogenesis in the striatum of PGC1 Lo rats, as demonstrated by an increase in the immunostaining for the mitochondrial marker HSP60, a chaperonin for protein transport and folding in the mitochondrial matrix (Fig. 4C).

PGC-1α induces perturbations in nigral dopaminergic neurons, ranging from the loss of dopaminergic markers to overt nigrostriatal degeneration

We next assessed the effect of PGC-1α expression on nigral neurons and their striatal projections. In the group PGC1 Lo, the expression of PGC-1α did not produce any significant loss of neurons positive for the dopaminergic markers vesicular monoamine transporter 2 (VMAT2) (Fig. 5A and E) and TH (Fig. 5B), or any loss of Nissl-stained nuclei in the SNpc (Fig. 5K) when compared with the control group non-coding vector (NCV) Lo, injected in the striatum with a non-coding vector. However, we noticed a decrease in staining intensity indicative of marker down-regulation (Fig. 5E). Indeed, we observed a reduction in VMAT2 (Fig. 5C and G), and TH immunoreactivity (Fig. 5D) at the level of the striatal nerve terminals (35.2 ± 2.6 and $37.3 \pm 2.5\%$, respectively). Interestingly, despite the fact that the vector had been injected in the striatum, PGC-1α did not produce any deleterious effect on striatal medium spiny neurons, as demonstrated by the normal intensity of the dopamine- and cyclic AMP-regulated phosphoprotein 32 (DARPP32) immunostaining (Fig. 5H). Therefore, PGC-1α appears to selectively impact on the expression of dopaminergic markers following intrastriatal vector injection.

In order to determine whether higher levels of PGC-1α may lead to neuronal loss, we analyzed the animals directly injected with the PGC-1α vector in the SNpc. At 3 months post-injection, PGC1 Hi rats displayed an overt loss of nigral neurons positive for VMAT2 ($45.5 \pm 7.1\%$; Fig. 5A and F) and TH ($50.7 \pm 6.1\%$, Fig. 5B) when compared with the group NCV Hi injected with a non-coding vector in the SNpc. Dopaminergic innervation in the striatum was similarly reduced. We measured a $63.0 \pm 7.1\%$ loss for VMAT2
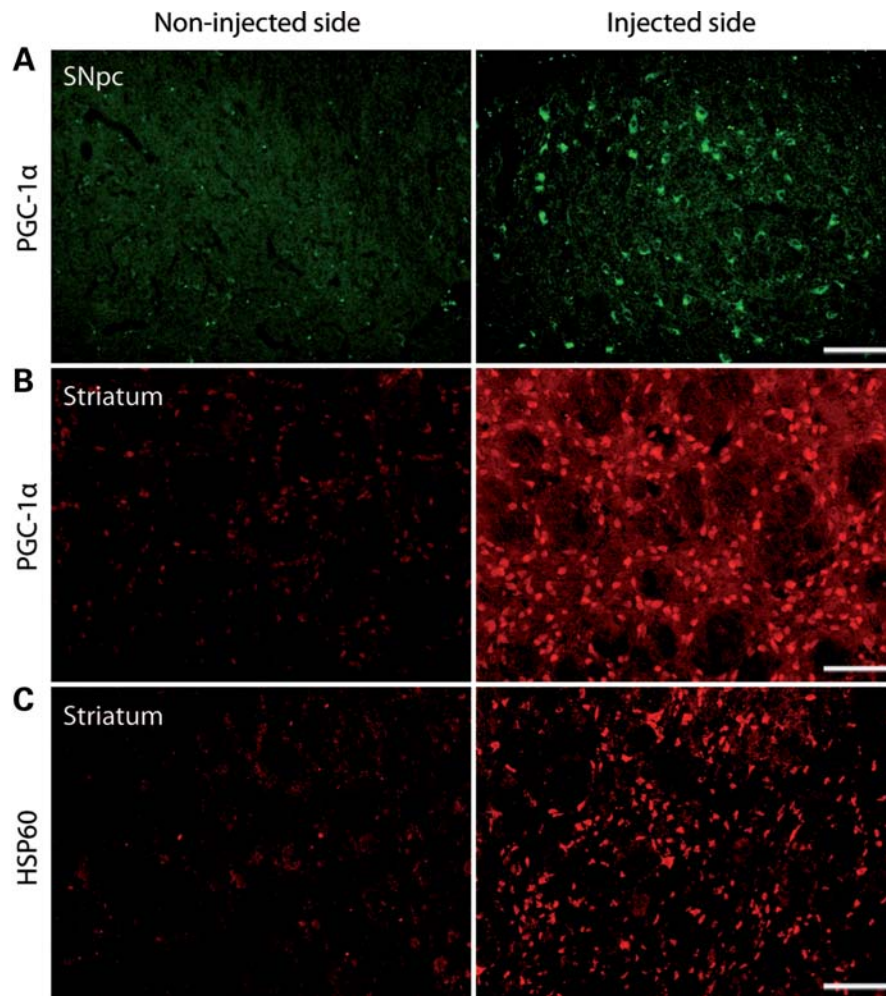
Figure 4. Overexpression of PGC-1α and long-term effects *in vivo*. (**A**) Nigral PGC-1α immunostaining at 3 months post-injection of an AAV2/6-PGC1 vector directly in the rat SNpc. (**B**) Striatal PGC-1α immunostaining at 3 months post-injection of an AAV2/6-PGC1 vector in the rat striatum. (**C**) HSP60 immunostaining showing mitochondrial biogenesis in the striatum of a rat injected with an AAV2/6-PGC1 in the striatum. For each immunostaining, the non-injected side (NInjS) is shown for comparison. Scale bar: 100 μm.

(Fig. 5C and I) and a 60.9 ± 7.5% loss for TH striatal immunoreactivity (Fig. 5D) when compared with the non-injected hemisphere. Again, the expression of the DARPP32 marker in striatal neurons remained intact (Fig. 5J).

Quantification of Nissl-stained neuronal nuclei in the SNpc revealed a 24.3 ± 4.2% reduction versus the non-injected side (Fig. 5K). In parallel to the loss of dopaminergic markers, we further explored if PGC-1α could induce any change in the expression of other neuronal markers. As PGC-1α has recently been demonstrated to control parvalbumin (PV) expression in interneurons (27), we immunostained striatal and ventral midbrain sections for PV. Indeed, we found a clear up-regulation of PV expression in the substantia nigra injected with the PGC-1α vector, when compared with the non-injected side or to the control group injected with a non-coding vector in the SNpc (Fig. 6A and B), suggesting that the overexpression of PGC-1α can perturb marker expression in surviving neurons. We observed the same up-regulation of PV expression in animals overexpressing PGC-1α in the striatum, when compared with the non-injected side or the control group

Table 1. Intranigral (PGC1 Hi, $n = 4$) versus intrastriatal (PGC1 Lo, $n = 4$) injection of the AAV2/6-PGC1 vector: fold increase in the level of PGC-1α mRNA expression in the *substantia nigra* and *striatum* of rats at 1 month post-injection

	Substantia nigra		Striatum	
	Mean	SEM	Mean	SEM
PGC1 Hi	399.5	182.2	0.4	0.3
PGC1 Lo	4.5	0.5	4.0	1.0

injected with a non-coding vector (Fig. 6C and D). Interestingly, the direct intrastriatal injection of the PGC-1α vector appears to selectively change PV expression and not the medium spiny neuronal marker DARPP32.

Altogether, these results highlight the effects of PGC-1α on the expression of dopaminergic markers and neuronal survival in the nigrostriatal system. Next, we sought to analyze how PGC-1α impacts on neuronal functions, such as DA synthesis. To determine these effects, we used only the cohort of rats
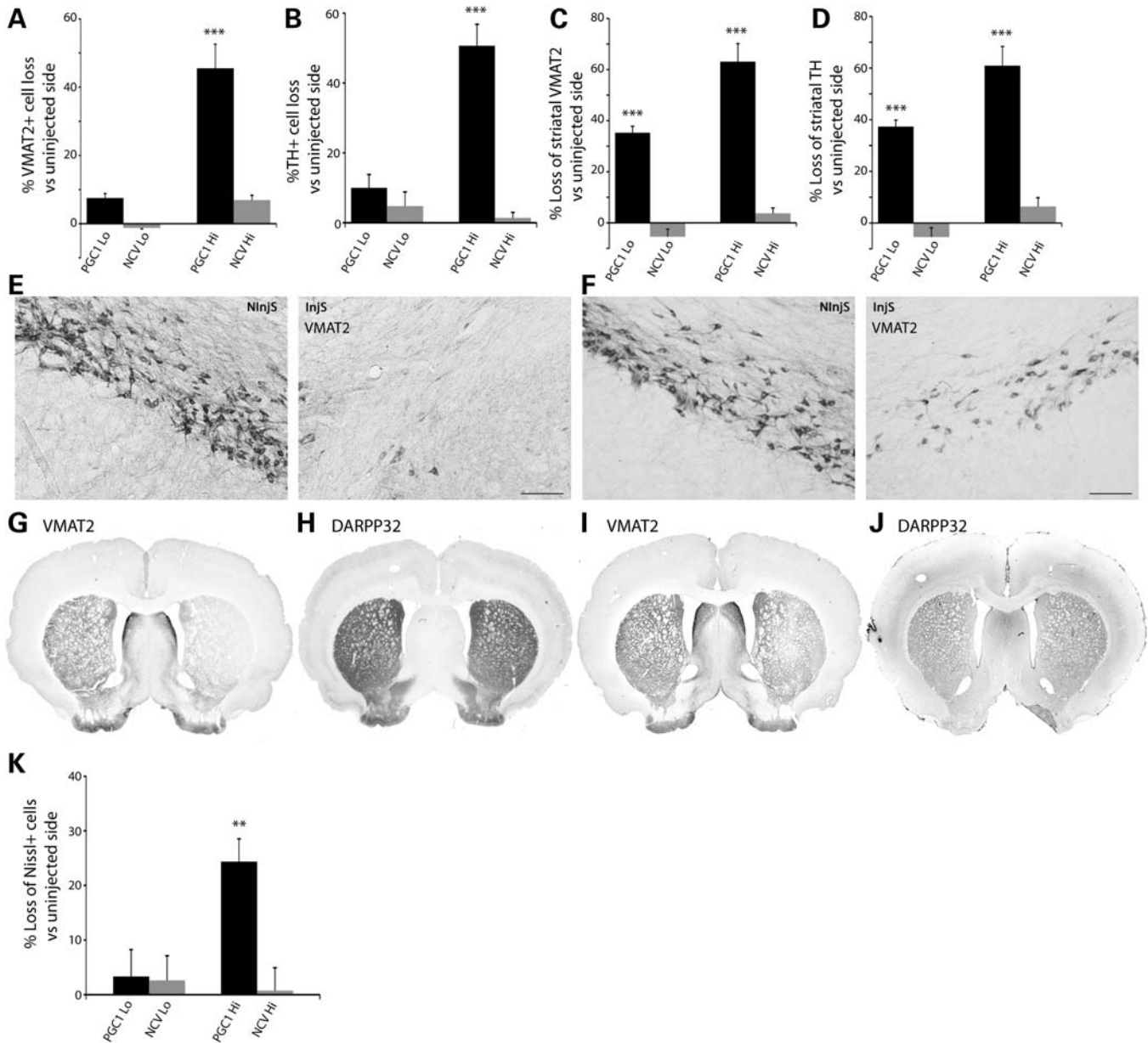
Figure 5. Loss of dopaminergic nigrostriatal markers in response to PGC-1α overexpression. (**A** and **B**) Loss of VMAT2-positive (A) and TH-positive (B) neurons in the SNpc of rats displaying either a moderate (PGC1 Lo) or a high level of PGC-1α overexpression (PGC1 Hi) in the SNpc at 3 months post-injection. Note the overt loss of VMAT2 and TH neurons in the PGC1 Hi condition. (**C** and **D**) Loss of striatal VMAT2 (C) and TH (D) immunoreactivity in PGC1 Lo and PGC1 Hi rats at 3 months post-injection. Note in both conditions, the loss of striatal dopaminergic markers. (**E** and **F**) Representative photomicrographs showing VMAT2-positive neurons in the SNpc of PGC1 Hi rats (E) and PGC1 Lo rats (F), when compared with the non-injected side (NInjS); scale bar: 100 μm. (**G** and **I**) Representative photomicrographs showing the loss of VMAT2 marker in the striatum of PGC1 Hi (G) and PGC1 Lo rats (I). In both conditions, striatal DARPP32 immunoreactivity remains intact (**H** and **J**—corresponding to PGC1 Hi and PGC1 Lo, respectively). (**K**) Stereological quantification of the percentage loss of Nissl-positive neurons in the SNpc.

with intrastriatal vector injections (PGC1 Lo), as these animals display a moderate level of PGC-1α overexpression in the SNpc with a minimal impact on neuronal survival.

PGC-1α overexpression impairs DA levels and DA turnover in the striatum

The level of DA and its metabolites were determined in extracts from striatal tissue. We compared rats injected in the striatum with either the PGC-1α vector, leading to a 4.5-fold increase in the level of PGC-1α mRNA in the SNpc (Table 1), or a control non-coding vector (AAV2/6-NCV), both at a dose of 6×10^7 TUs. When compared with the non-injected hemisphere, we measured a clear reduction in the striatal DA level ($42.9 \pm 1.7\%$) only in the PGC1 Lo group (Fig. 7A), consistent with the loss in TH expression. The levels of the DA metabolites DOPAC ($74.6 \pm 3.3\%$) and HVA ($56.6 \pm 3.2\%$) appeared to be further reduced when
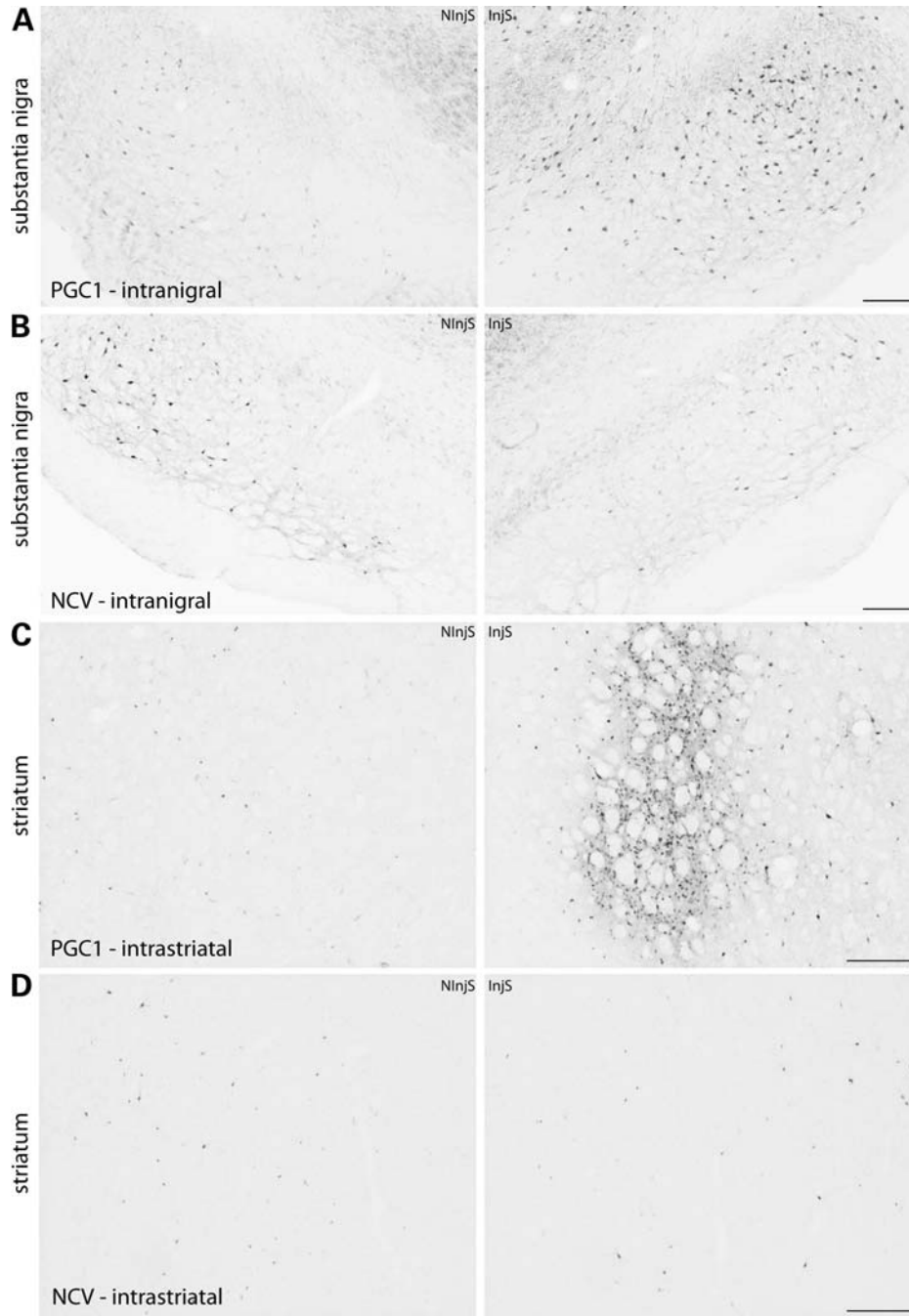
Figure 6. PGC-1α up-regulates PV expression in the *substantia nigra* and *striatum*. Immunostaining demonstrating an increase in the amount of PV-positive neurons in the injected SNpc and *reticulata* of rats injected with AAV2/6-PGC1 in the SNpc (**A**). No change in PV expression in rats injected with a non-coding vector in the SNpc (**B**). PGC1 and NCV Hi; scale bar: 200 μm. A clear up-regulation of the striatal interneuron marker PV is found in rats injected with AAV2/6-PGC1 in the striatum (**C**), in contrast to rats similarly injected with a non-coding vector (**D**). PGC1 and NCV Lo; scale bar: 250 μm.

compared with the non-injected hemisphere. In the control group injected with a non-coding vector, the level of DA and metabolites remained similar in both the injected and non-injected striata.

We assessed DA turnover by calculating the ratio between metabolites and total DA content: (DOPAC + HVA)/DA. In response to PGC-1α, we observed a significant increase in the relative abundance of DA metabolites (Fig. 7B). In the striata injected with the AAV2/6-NCV vector, DA turnover remained similar to the non-injected side. Increased DA turn-over induced by PGC-1α could lead to increased production of hydrogen peroxide associated with oxidative stress.

Consistent with the reduction in striatal DA observed at 3 months post-injection, PGC1 Lo animals showed a rotational behavior induced by amphetamine, reaching 2.5 ± 1.0 ipsiver-sive turns per min, significantly increased from 0.5 ± 0.6
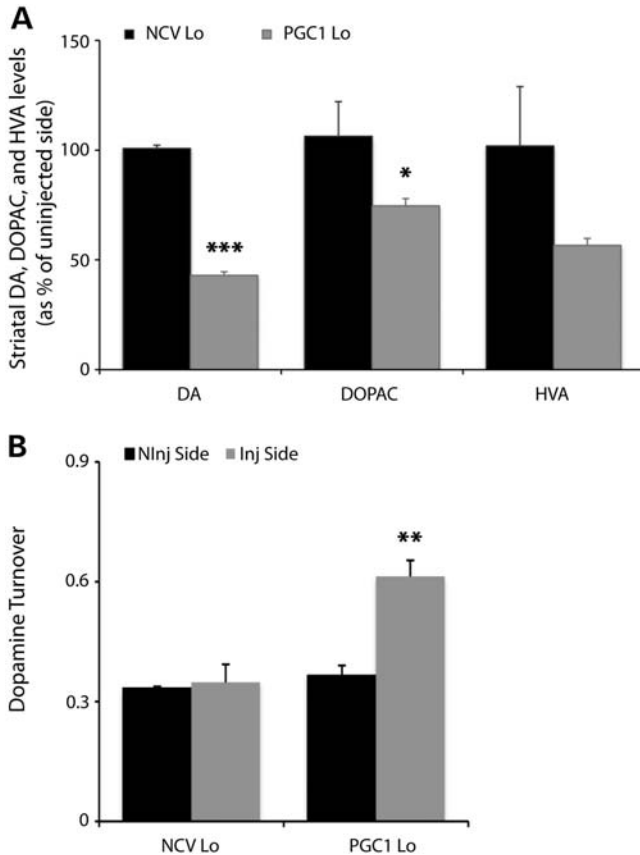
Figure 7. Depletion of DA and metabolites and increased DA turnover. (**A**) Total striatal content of DA, DOPAC and HVA in the non-injected and injected hemispheres of PGC1 Lo and NCV Lo rats at 3 months post-injection. Results are expressed as the ratio of metabolite concentration in the injected versus non-injected hemisphere. Note the significant decrease in striatal levels of DA and metabolites in PGC1 Lo rats. Student's *t*-test: NCV Lo: $n = 2$, PGC1 Lo: $n = 5$; $*P < 0.05$, $***P < 0.001$. (**B**) PGC1 Lo rats show higher DA turnover. DA turnover is determined as ([DOPAC]+[HVA])/[DA]. Student's *t*-test: NCV Lo, $n = 2$; PGC1 Lo, $n = 5$, $**P < 0.01$.

contraversive turns per min before vector injection ($P < 0.01$, paired *t*-test). The same animals displayed neither any apomorphine-induced rotations, nor any spontaneous asymmetry in forepaw use.

As suggested by the observed loss of dopaminergic markers in the striatum, PGC-1α induced a clear decrease in DA levels, in part due to an increase in the turnover rate.

In response to PGC-1α, nigral neurons show a clear defect in retrograde labeling following striatal injection of the fluorogold tracer

As the loss of dopaminergic markers appeared most evident in striatal fibers following intrastriatal injection of the PGC-1α vector (PGC1 Lo), we further explored nigrostriatal axonal transport in these conditions. Three months post-injection of the vector, animals were injected in the striatum with the neuroanatomical retrograde tracer fluorogold and sacrificed 5 days later. As expected, we observed a fluorogold signal in the majority of the nigral neurons in the animals injected with the control vector AAV2/6-NCV, demonstrating an

intact capacity to retrogradely transport the tracer (Fig. 8). In stark contrast, no fluorogold signal could be detected in TH-positive neurons on the hemisphere injected with 6×10^7 TUs of the AAV2/6-PGC-1α vector. Considering the significant proportion of neuronal cell bodies and striatal axonal fibers that are still present in these conditions, this result denotes impaired synaptic uptake or disruption of the axonal retrograde transport in response to PGC-1α.

Altogether, these results demonstrate that the level of PGC-1α impacts on the mitochondrial function of neurons from the ventral midbrain and thereby affects nigrostriatal function in normal adult animals. Next, we sought to explore the effect of PGC-1α overexpression in pathologic conditions related to PD. The expression of human αSyn using AAV vectors was used to specifically induce pathological changes in the rat nigrostriatal system.

Nigrostriatal PGC-1α overexpression does not prevent the degeneration of nigral dopaminergic neurons expressing human αSyn

We have previously reported that the expression of human αSyn in the rat SNpc using AAV2/6 vectors leads to mild neurodegeneration (28). In order to assess the effect of PGC-1α on αSyn pathology, adult rats were injected in the SNpc with AAV2/6 encoding either human wild-type αSyn (αSynWT) or the PD-associated mutant A53T, at a dose of 2×10^7 TUs. These conditions induce progressive nigrostriatal neurodegeneration associated with moderate behavioral impairments (M. Gaugler *et al.*, manuscript in preparation). In the same time, the animals were injected in the ipsilateral striatum with the AAV2/6-PGC-1α vector to induce a moderate expression of PGC-1α in the SNpc. Control rats received a similar injection of the non-coding vector.

The activity of both forepaws was monitored in the cylinder test, where the animals showed a reduction in the use of the left forepaw in response to αSyn expression (Fig. 9A and B). Overall, we did not observe any significant changes in spontaneous motor activity in response to PGC-1α. Although the animals injected with the PGC-1α displayed a nonsignificant trend towards improved motor symmetry at 1 month for αSynWT, and until 2 months for the A53T mutant, motor activity of the left forepaw then deteriorated and reached the same level as control animals expressing αSyn only.

However, we noticed a significant difference in amphetamine-induced rotations (Fig. 9C). Indeed, when compared with the animals expressing only αSyn, the rats co-injected with the PGC-1α vector showed ipsiversive behavior, which likely reflects the reduction in striatal DA due to PGC-1α. Overall, the amphetamine-induced rotational response to both αSyn and PGC-1α remained weak.

At 3 months post-injection, we analyzed the effect of PGC-1α on nigral dopaminergic neurons expressing human αSyn. PGC-1α did not prevent the loss of VMAT2-positive nigral neurons induced by expression of either the wild-type or A53T forms of αSyn. In animals expressing the A53T mutant, the cell loss appeared similar with both PGC-1α and the non-coding vector (Fig. 9D). In the αSynWT condition, there was a trend towards increased loss of VMAT2-positive
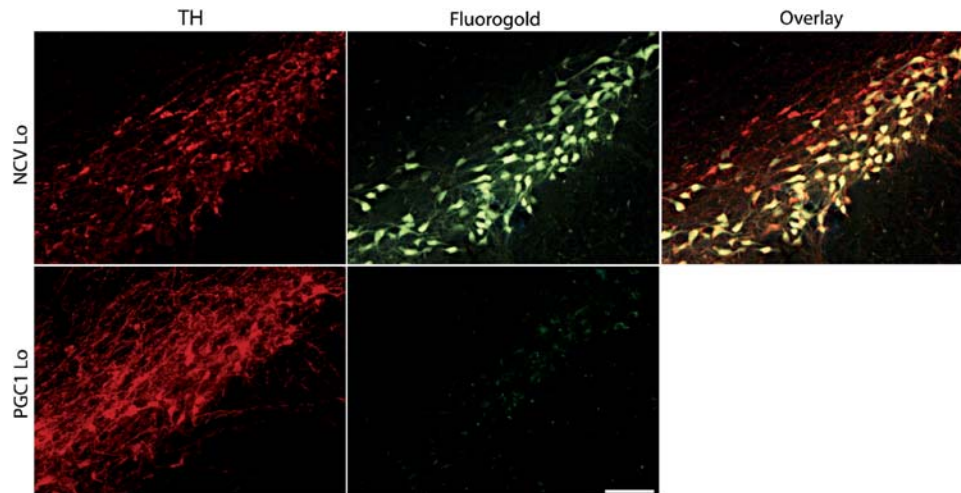
Figure 8. Absence of fluorogold retrograde labeling in nigral dopaminergic neurons overexpressing PGC-1α. Immunostaining for TH expression and fluorogold uptake at 3 months post-injection of either PGC-1α or non-coding vector. Note the absence of fluorogold signal in the SNpc of PGC1 Lo rats, indicative of impaired uptake or retrograde transport of the tracer. PGC1 and NCV Lo; scale bar: 100 μm.

neurons with the PGC-1α vector, versus the non-injected side (αSynWT + PGC1: 29.3 ± 4.7%, αSynWT + NCV: 18.9 ± 3.2%). However, the difference did not reach statistical significance ($P = 0.14$; Fig. 9D).

In the striatum, we again observed a significant increase in the loss of VMAT2 immunoreactivity in conditions of PGC-1α overexpression (Fig. 9E). The effect was similar when PGC-1α was combined with either αSynWT (αSynWT + PGC1: 39.6 ± 3.6%, versus αSynWT + NCV: 15.9 ± 4.9%) or the A53T mutant (A53T + PGC1: 43.0 ± 5.1%, versus A53T + NCV: 15.3 ± 7.2%).

Overall, moderate levels of PGC-1α overexpression in normal rats lead to cellular and mitochondrial changes which selectively interfere with the dopaminergic phenotype of nigral neurons. In pathologic conditions induced by human αSyn, PGC-1α overexpression does not oppose neurodegeneration.

DISCUSSION

Although PGC-1α is considered a promising target for neurodegenerative disease associated with mitochondrial dysfunction, few studies have assessed the effect of PGC-1α overexpression in the central nervous system. In a mouse model for amyotrophic lateral sclerosis, transgenic expression of PGC-1α has protective effects against mutated SOD1 toxicity (23,24). Here, we overexpress PGC-1α in the nigrostriatal system using an AAV vector which primarily targets striatal neurons, and retrogradely infects nigral dopaminergic neurons. We find that PGC-1α expression in the SNpc selectively impacts on the dopaminergic function, leading to reduced expression of dopaminergic markers, increased DA turnover, impaired retrograde axonal transport and neuronal loss.

In primary cultures derived from the ventral midbrain, PGC-1α affects mitochondrial function in a time-dependent manner. PGC-1α induces mitochondrial biogenesis, consistent with increased oxidative phosphorylation reflected by an augmentation in oxygen consumption. However, neuronal metabolic activity changes over time in response to PGC-1α. Indeed, although the basal cell respiration rate remains higher than control, less oxygen is used for ATP production. Mitochondria display a significant reduction in their reserve respiratory capacity and a significant decrease in membrane potential. The uncoupling of oxidative phosphorylation dedicated to ATP production that progressively appears in response to PGC-1α could be seen as an adaptive mechanism to lessen the production of ROS. As mitochondrial metabolism is recognized as the most important source of ROS (29), mitochondrial biogenesis is expected to increase oxidative stress in neurons. Therefore, the progressive alteration of the mitochondrial function may limit ROS production despite the observed increase in the mitochondrial mass.

Here, we find that the neuronal response to PGC-1α is associated with the clear up-regulation of several genes implicated in the loss of mitochondrial membrane potential and oxidative stress resistance (*Slc25a4*, *UCP3*, *Bnip3*, *Sod2*). In particular, Slc25a4, also known as ADP/ATP translocase 1 (ANT1), is a major mitochondrial constituent and a core component of the mitochondrial permeability transition pore. ANT1 is responsible for the transfer of ADP and ATP through the inner mitochondrial membrane, a process highly dependent on the proton gradient. ANT1 overexpression has been reported to induce rapid cell death with a concomitant decrease in mitochondrial membrane potential (30,31). UCP3, which is activated by superoxide, increases mitochondrial proton conductance and dissipates the membrane gradient (32,33). Bnip3 is a pro-apoptotic protein, member of the Bcl-2 family. Upon activation, Bnip3 inserts into the mitochondrial outer membrane, which causes opening of the mitochondrial permeability transition pore, loss of mitochondrial potential, generation of ROS and necrosis (34). Sod2, a manganese-binding protein in the mitochondrial matrix, is critically involved in superoxide detoxification (35). The up-regulation of Sod2 may contribute to neuronal survival in conditions of increased ROS production. Overall, the pattern of gene expression changes
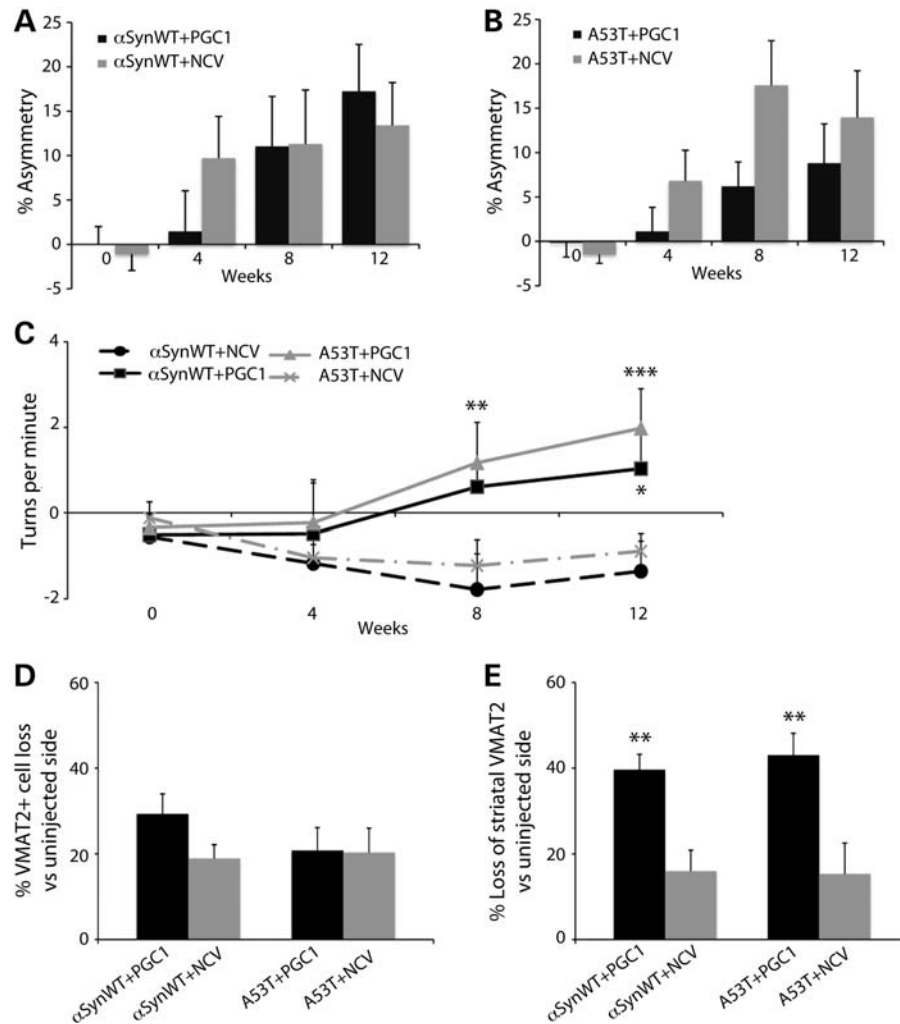
Figure 9. Loss of dopaminergic markers and behavioral assessment in response to PGC-1α overexpression in rats expressing human αSyn. Rats were injected in the SNpc with AAV2/6 vectors encoding either human αSynWT or the A53T mutant. The animals were simultaneously injected in the striatum with an AAV2/6 vector encoding PGC-1α or a NCV to ensure a moderate expression in the SNpc. (**A**–**C**) To assess motor asymmetry, forepaw activity was measured in the cylinder test (A and B) and ipsiversive rotations were measured following amphetamine administration (C). In the cylinder test, note the progressive development of an asymmetry in forepaw use typically observed following unilateral expression of αSynWT or A53T (repeated measure ANOVA, time effect: $P < 0.005$). PGC-1α does not significantly rescue the behavioral phenotype induced by αSyn in the cylinder test. In amphetamine-induced rotational behavior, PGC-1α induces a significant change towards ipsiversive rotations (one-way ANOVA with Newman–Keuls *post hoc* test; $n = 10$ in each group: $^{*}P < 0.05$, $^{**}P < 0.01$ and $^{***}P < 0.001$). (**D** and **E**) PGC-1α overexpression does not protect against αSyn toxicity, as demonstrated by the loss of nigral VMAT2-positive neurons (D) and striatal VMAT2-positive fibers (E); $n = 10$ animals per group. Student's *t*-test, $^{**}P < 0.01$.

suggests a cellular response to oxidative stress, coherent with the observed increase in the basal rate of oxidative phosphorylation.

There is converging evidence for alterations of axonal trafficking in response to PGC-1α overexpression in midbrain dopaminergic neurons. Striatal fluorogold injections reveal a complete absence of tracer labeling in nigral cell bodies, demonstrating either impaired synaptic uptake or reduced retrograde transport of the tracer. In addition, we observed consistent changes in the expression of several genes related to axonal transport and mitochondrial movement along axons, such as up-regulation of the *Nefl* and *Rhot1*. Nefl is implicated in the localization of mitochondria, which depends on the docking of mitochondria to microtubules and

neurofilaments (36). As the direction of mitochondrial transport along axons also depends on organelle membrane potential (37), it is possible that the expression of PGC-1α produces major perturbations in organelle trafficking, which may ultimately cause axonal degeneration and cell death.

In rats injected with the AAV-PGC-1α vector, we find that PGC-1α overexpression opposes nigral dopaminergic function. The effect is progressive, as demonstrated by the slow development of amphetamine-induced rotational behavior, and primarily affects nigrostriatal axonal projections. As part of the mechanisms opposing dopaminergic function in response to PGC-1α, we observed an increase in DA turnover. The expression of monoamine oxidase B present on the mitochondrial outer membrane is regulated by

PGC-1α and ERRα (38). DA enzymatic catabolism by mono-amine oxidase produces hydrogen peroxide causing oxidative stress and protein oxidation (39). Increased DA oxidation may therefore contribute to the selective demise of nigral neurons. The effect of PGC-1α on the survival of nigral dopaminergic neurons appears to highly depend on its level of overexpression. While striatal injections of the PGC-1α vector lead to the down-regulation of dopaminergic markers, intranigral vector injections cause overt neuronal loss. Furthermore, we find that injections of the PGC-1α vector upregulates PV, a marker for GABAergic interneurons. It has already been reported that PGC-1α can induce PV expression in neuroblastoma cells (27). In the brain, PGC-1α, PV and mitochondria coordinately regulate Ca^{2+} homeostasis in a cell-specific manner. Interestingly, mice ectopically expressing PV in neurons show alterations in Ca^{2+} homeostasis and a reduced mitochondrial volume (40).

Interestingly, PGC-1α expression in the striatum does not affect GABAergic medium spiny neurons, highlighting the selective vulnerability of dopaminergic neurons to the changes induced by PGC-1α. Therefore, DA could represent an important mediator in potentiating PGC-1α toxicity in the nigrostriatal system. The loss of striatal dopaminergic markers and nigral degeneration are most likely due to mitochondrial dysfunction. Mitochondria are crucial organelles for the energy-demanding process of synaptic neurotransmission. The distribution and trafficking of mitochondria affect neurotransmitter synthesis, release and recycling through energy metabolism and synaptic calcium modulation (41–43). Synaptic mitochondria are more sensitive to a decrease in oxidative phosphorylation (44). The cellular morphology of nigral dopaminergic neurons, with long and highly branched striatal neurites, as well their exposure to calcium signaling (45) may therefore contribute to the observed impact of PGC-1α.

Altogether, this study emphasizes the importance of tightly controlling the expression of PGC-1α in dopaminergic neurons. PGC-1α is a powerful regulator of energy metabolism and its overexpression has already proved similarly detrimental in muscle and heart tissues. Cardiac PGC-1α overexpression causes severe abnormalities in the myocyte architecture due to extensive mitochondrial proliferation (46,47). In the skeletal muscle, PGC-1α overexpression enhances not only mitochondrial biogenesis but also respiration uncoupling, leading to muscle atrophy (48). However, PGC-1α expression within physiological limits does indeed improve insulin sensitivity both in normal and insulin-resistant skeletal muscle (49).

In the present study, we show that the function and survival of nigral dopaminergic neurons are selectively vulnerable to the progressive metabolic changes caused by the overexpression of PGC-1α, to levels beyond those observed under normal physiological circumstances. In the context of PD, mounting evidence highlights the critical links that exist between the pathologic process and PGC-1α activity (20,21). Notably, the E3 ubiquitin ligase parkin has recently been found to control the level of PARIS, a transcriptional repressor of PGC-1α (50). Pioglitazone, an agonist of PPARγ which has been shown to induce PGC-1α activity, is neuroprotective in the MPTP model of PD (51–53). Based on these effects and

on the increasing evidence for the critical role of PGC-1α in the pathology, a phase II clinical trial has been launched in PD patients to assess the effects of pioglitazone on the early phase of the disease. It will be of interest to determine the effects of this compound in the disease context where a pre-existing down-regulation of PGC-1α has to be expected. However, it should be noted that Breidert *et al.* (51) also found a significant reduction in striatal DA in pioglitazone-treated mice prior to MPTP intoxication, further amplifying the notion that up-regulating PGC-1α in normal animals may impact on the dopaminergic function.

Although PGC-1α expression should be carefully controlled, our data confirm the crucial role of this transcriptional co-activator in the function and survival of dopaminergic neurons. In PD, it appears therefore critical to design therapeutic strategies maintaining a tight and physiological regulation of PGC-1α expression in the nigrostriatal system.

MATERIALS AND METHODS

Plasmid construction

Human WT (nucleotides 46–520, GeneBank accession no. NM_000345) and A53T αSyn and mouse PGC-1α (nucleotides 35–2428, GeneBank accession no. BC066868) were inserted into the pAAV-pgk-MCS backbone, modified from the serotype 2 pAAV-cmv-MCS (Agilent, La Jolla, CA, USA) using standard cloning procedures.

Recombinant AAV2/6 production and titration

Recombinant pseudotyped rAAV2/6 were produced, purified and titrated as described previously (54). A stuffer sequence was included in the plasmid pAAV-pgk-MCS to generate a non-coding vector with a comparable genome size. Vector titration has been determined as described previously (54). The measured titers were as follows: AAV-pgk-αSynWT 9.0×10^{10} TU/ml; AAV-pgk-A53T 5.0×10^{10} TU/ml; AAV-pgk-MCS (non-coding vector) 4.5×10^{10} TU/ml; AAV-pgk-PGC-1α 8.7×10^{10} TU/ml; 7.4×10^{10} TU/ml; AAV-cmv-GFP 1.5×10^{10} TU/ml and AAV-cmv-MitoDsRed 8.9×10^{9} TU/ml.

Stereotaxic unilateral injection into the SNpc and striatum of rats

Female adult Sprague-Dawley (Charles River Laboratories, France), weighing ∼200 g were housed in a 12 h light/dark cycle, with *ad libitum* access to food and water, in accordance with Swiss legislation and the European Community Council directive (86/609/EEC) for the care and use of laboratory animals. AAV vectors were injected unilaterally in the right hemisphere. Stereotaxic injections into the SNpc were performed as described previously (54). In the striatum, virus suspension was injected in two deposits along three needle tracts at the following coordinates: anterior–posterior (AP)/mediolateral (ML) relative to bregma/dorsoventral (DV) relative to skull surface 1.7 mm/−2.8 mm/−5.8 mm and −4.2 mm, +0.7 mm/−3.2 mm/−6.3 mm and −5 mm, −0.4 mm/−3.8 mm/−6.2 mm and −5 mm. Two microliters

of rAAVs at a concentration of 5×10^9 TU/ml were injected per site using a 10 μl Hamilton syringe with a 34-gauge blunt tip needle at a speed of 0.2 μl/min, with an automatic pump (CMA Microdialysis, Sweden). The more ventral site in each needle tract was injected first and the needle was left in place for 2 min before slowly moving to the more dorsal site. After injection, the needle was left for an additional 5 min before slowly being withdrawn. To study the retrograde transport, a fluorogold preparation was injected at one site in the striatum 5 days before sacrifice. The striatum was targeted at the following coordinates: AP +0.2, ML −3, DV +5. The concentration of the fluorogold was at 2% in normal sterile 0.9% saline.

Primary neuronal culture from mouse ventral midbrain

The protocol used for the preparation of the primary neuronal culture from mouse ventral midbrain was adapted from reference (55). The ventral midbrain portion of embryonic brains (E16) was dissected out under a microscope and kept in warm Hank's buffered salt solution (HBSS) wo Ca^{2+} and Mg^{2+}. Mesencephalic tissues were isolated and dissociated with gentle mechanical trituration, followed by an enzymatic digestion in Trypsin/ethylenediaminetetraacetic acid diluted in warm HBSS w/o Ca^{2+} and Mg^{2+} (1:1) for 20 min at 37°C. Enzyme inactivation is done by adding the Neurobasal medium supplemented with 10% heat inactivated fetal bovine serum, GlutaMAX 1× and 1% Pen-Strep (dissociation medium). Dissociated cells were centrifuged 5 min at 800 rpm and resuspended in the dissociation medium. Cells were, then, filtered (40 μm) and centrifuged 5 min at 800 rpm. Neurons were, finally, resuspended in the plating medium: neurobasal medium low glucose supplemented with B27 1×, GlutaMAX 1×, 20 mM pyruvate and 1% Pen-Strep. The cell concentration and the viability were determined using a classic dye exclusion method (Trypan Blue). Neurons were seeded into 24-well culture plates precoated with poly-D-lysine (100 μg/ml) and laminin (20 μg/ml) at 7.5×10^4 cells per well. Plates were maintained at 37°C in a humidified atmosphere of 5% CO_2. Seven-day-old cultures were used for AAV infections. For AAV-mediated transduction, each 24-well was infected with a viral dose of 6×10^6 TUs.

Flow cytometry

Primary midbrain neurons were seeded in precoated 24-well plates at 1×10^5 cells per well and cultured for 7 days in 37°C/5% CO_2 incubators. Neurons were then infected with an AAV2/6 coding for PGC-1α or GFP at a dose of 6×10^6 TUs. Three days later, neurons were infected with a vector encoding the MitoDsRed fluorescent protein at a dose of 6×10^6 TUs. Two days later, cultures were harvested and neurons were carefully collected with a cell scraper. Neurons were fixed using 4% paraformaldehyde for 15 min at RT. After two washes in 1× phosphate buffered saline, cell PE-Cy5 fluorescence was measured using a flow cytometer (CyAn ADPS analyzer, Beckman Coulter).

Measurements of oxygen consumption

Oxygen measurements were made using the XF24 Extracellular Flux Analyzer (Seahorse Bioscience, Billerica, MA, USA). Primary midbrain neurons were seeded in pre-coated XF24-well microplates at 7.5×10^4 cells per well and cultured for 7 days in 37°C/5% CO_2 incubators. Neurons were then infected with an AAV2/6 coding for PGC-1α or a non-coding vector at a dose of 6×10^6 TUs. The basal respiration rate was measured during 60 min. Assay protocols including compound injection are preprogrammed through an excel template. Compounds of interest (Oligomycin and FCCP) were loaded in the drug delivery system of sensor cartridge before calibration. The assay cartridge was first placed into XF Analyzer to allow automatic calibration of optical sensors. Then, the cell culture plate was inserted into the instrument. Basal OCRs were measured six times before drug addition. Drugs that have been preloaded into the drug delivery chambers of the assay cartridge were then pneumatically injected, sequentially, into the media in each well. After mixing, post-exposure OCR measurements were made three times. The effects on cellular respiration rates were measured during 60 min after addition of oligomycin and during 30 min after addition of FCCP.

Measurements of mitochondrial depolarization

Studies of mitochondrial depolarization have been made with MitoProbe[TM] JC-1 Assay Kit (Invitrogen). Primary midbrain neurons were seeded in precoated 24-well plates at 1×10^5 cells per well and cultured for 7 days in 37°C/5% CO_2 incubators. Neurons were then infected with an AAV2/6 coding for PGC-1α or a non-coding vector at a dose of 6×10^6 TUs. Neurons were incubated 20 min with 2 μM JC-1, and then washed twice with warm Neurobasal medium without phenol red. Plates were analyzed on a fluorometer (Tecan Safire2 microplate reader) using wavelengths at 497 nm for excitation and 527 nm (green fluorescence) and 597 nm (red fluorescence) for emission.

RNA extraction and RT–QPCR

In vitro studies. Primary midbrain neurons were seeded in precoated 24-well plates at 1×10^5 cells per well and cultured for 7 days in 37°C/5% CO_2 incubators. Neurons were then infected with an AAV2/6 coding for PGC-1α or a non-coding vector at a dose of 6×10^6 TUs. Five and 7 days post-infection, cultures were harvested and neurons were collected with a cell scraper. Total RNA was isolated with RNAeasy Mini Kit (Qiagen Inc., Valencia, CA, USA). cDNA was prepared using RT[2] First Strand Kit (SA Biosciences, Frederick, MD, USA). The expression levels of 84 mitochondrial genes implicated in biogenesis and function and 12 housekeeping genes including internal controls were measured by quantitative RT–PCR using RT[2] Profiler[TM] PCR Array (SA Biosciences). Assays were run on a ABI 7900HT 384-Well Block (Applied Biosystems, Foster City, CA, USA) using the following cycling conditions (10 min at 95°C, then 15 s at 95°C and 1 min at 60°C for 40 cycles). Four independent pairwise comparisons (PGC1 versus NCV) were performed at two time points to evaluate scored differences in gene

changes. An integrated web-based software package for the PCR Array System was used to perform ΔΔCt-based fold change calculations from the uploaded raw threshold cycle data.

In vivo *studies*. To determine the level of PGC-1α mRNA expression in the SN and the striatum, rats were killed by decapitation at 3 weeks after rAAV injection ($n = 4$ per group). Striata and SN were rapidly dissected. Total RNA was isolated with an RNAeasy Mini Kit (Qiagen). cDNA was prepared using a Omniscript Reverse Transcription Kit. Briefly, total RNA (50 ng) was reverse transcribed in a final volume of 20 μl with OligodT primers at 37°C for 1 h according to the manufacturer's instructions. The expression level of PGC-1α was measured by RT–QPCR using SybrGreen assays. The genes ACTB and B2M were used as endogenous controls. We used Quantitect Primer Assays (Qiagen) to quantify expression of these three genes. Each assay was run in duplicate, with the Rotor-Gene Sybr Green PCR Kit (Qiagen) on a Rotor-Gene Cycler using the following cycling conditions: 5 min at 95°C, then 5 s at 95°C and 10 s at 60°C for 40 cycles.

Each replicate cycle threshold (Ct) was normalized to the average Ct of the two endogenous controls on a per sample basis. The comparative Ct method was used to calculate relative levels of PGC-1α expression, as described previously (56,57).

Immunohistological analyses and quantification of nigrostriatal lesions

Rats were sacrificed and tissue processed as described before (28,54). Primary antibodies used in this study were anti-TH (Rabbit IgG, 1:1000; AB152, Chemicon), anti-VMAT2 (rabbit IgG, 1:2000; AB1767, Chemicon), anti-DA and cyclic AMP-regulated phosphoprotein, relative molecular mass 32000 (DARPP32) (Rabbit IgG, 1:1000; AB1656, Chemicon), anti-PV (rabbit IgG, 1:6000; PV-28 Swant, Bellinzona, Switzerland), anti-PGC-1α (rabbit IgG, 1:1000; generous gift from Dan Kelly, Burnham Institute for Medical Research, Orlando, FL, USA) and anti-heat shock protein 60 kDa (HSP60) (mouse IgG, 1:250; LK-1, Calbiochem). For fluorescence labeling, we used secondary antibodies conjugated to Alexa Fluor-488 (1:500; Invitrogen), Cy3 (1:1000; Jackson ImmunoResearch). For bright-field microscopy, we used biotinylated goat anti-rabbit secondary antibody (1:200; Vector Laboratories). Stereological estimates of Nissl-positive and TH-positive nigral neurons were made as described previously (58). For quantification of VMAT2-positive neurons, the percentage of neuronal loss was determined in a blinded fashion by counting nigral dopaminergic neurons using bright-field microscopy, as described previously (28,54). Of note, stereological estimates and neuron counting on the same groups of samples yielded identical results. The extent of striatal dopaminergic innervation was measured by determining the optical density on immunostained slices (54).

HPLC analysis of DA and DA metabolites

Contents of DA and DA metabolites were measured as described before (54). Results are expressed as a percentage of the non-injected hemisphere.

Behavioral analysis

Cylinder test and amphetamine-induced rotation test were performed as described previously (54), before virus injection and at monthly intervals post-surgery. In the cylinder test, only the measurements with a minimum of 20 touches were included in the analysis.

Statistical analysis

Data are expressed as average ± standard error of the mean (SEM). Statistical analysis was performed using the Statistica software (StatSoft Inc., OK, USA). Level of significance was set at 0.05. Applied statistical tests are indicated in the figure legends.

REFERENCES

1. Schon, E.A. and Manfredi, G. (2003) Neuronal degeneration and mitochondrial dysfunction. *J. Clin. Invest.*, **111**, 303–312.
2. Beal, M.F. (2005) Mitochondria take center stage in aging and neurodegeneration. *Ann. Neurol.*, **58**, 495–505.
3. Jones, D.C. and Miller, G.W. (2008) The effects of environmental neurotoxicants on the dopaminergic system: a possible role in drug addiction. *Biochem. Pharmacol.*, **76**, 569–581.
4. Vila, M., Ramonet, D. and Perier, C. (2008) Mitochondrial alterations in Parkinson's disease: new clues. *J. Neurochem.*, **107**, 317–328.
5. Clark, I.E., Dodson, M.W., Jiang, C., Cao, J.H., Huh, J.R., Seol, J.H., Yoo, S.J., Hay, B.A. and Guo, M. (2006) Drosophila pink1 is required for mitochondrial function and interacts genetically with parkin. *Nature*, **441**, 1162–1166.
6. Deng, H., Dodson, M.W., Huang, H. and Guo, M. (2008) The Parkinson's disease genes pink1 and parkin promote mitochondrial fission and/or inhibit fusion in Drosophila. *Proc. Natl Acad. Sci. USA*, **105**, 14503–14508.
7. Koh, H. and Chung, J. (2010) PINK1 and Parkin to control mitochondria remodeling. *Anat. Cell Biol.*, **43**, 179–184.
8. Devi, L., Raghavendran, V., Prabhu, B.M., Avadhani, N.G. and Anandatheerthavarada, H.K. (2008) Mitochondrial import and accumulation of alpha-synuclein impair complex I in human dopaminergic neuronal cultures and Parkinson disease brain. *J. Biol. Chem.*, **283**, 9089–9100.

9. Martin, L.J., Pan, Y., Price, A.C., Sterling, W., Copeland, N.G., Jenkins, N.A., Price, D.L. and Lee, M.K. (2006) Parkinson's disease alpha-synuclein transgenic mice develop neuronal mitochondrial degeneration and cell death. *J. Neurosci.*, **26**, 41–50.

10. Parihar, M.S., Parihar, A., Fujita, M., Hashimoto, M. and Ghafourifar, P. (2008) Mitochondrial association of alpha-synuclein causes oxidative stress. *Cell Mol. Life Sci.*, **65**, 1272–1284.

11. Lashuel, H.A., Petre, B.M., Wall, J., Simon, M., Nowak, R.J., Walz, T. and Lansbury, P.T. Jr (2002) Alpha-synuclein, especially the Parkinson's disease-associated mutants, forms pore-like annular and tubular protofibrils. *J. Mol. Biol.*, **322**, 1089–1102.

12. Puigserver, P. (2005) Tissue-specific regulation of metabolic pathways through the transcriptional coactivator PGC1-alpha. *Int. J. Obes. (Lond.)*, **29** (Suppl. 1), S5–S9.

13. Finck, B.N. and Kelly, D.P. (2006) PGC-1 coactivators: inducible regulators of energy metabolism in health and disease. *J. Clin. Invest.*, **116**, 615–622.

14. Schreiber, S.N., Emter, R., Hock, M.B., Knutti, D., Cardenas, J., Podvinec, M., Oakeley, E.J. and Kralli, A. (2004) The estrogen-related receptor alpha (ERRalpha) functions in PPARgamma coactivator 1alpha (PGC-1alpha)-induced mitochondrial biogenesis. *Proc. Natl Acad. Sci. USA*, **101**, 6472–6477.

15. Wu, Z., Puigserver, P., Andersson, U., Zhang, C., Adelmant, G., Mootha, V., Troy, A., Cinti, S., Lowell, B., Scarpulla, R.C. *et al.* (1999) Mechanisms controlling mitochondrial biogenesis and respiration through the thermogenic coactivator PGC-1. *Cell*, **98**, 115–124.

16. St-Pierre, J., Drori, S., Uldry, M., Silvaggi, J.M., Rhee, J., Jager, S., Handschin, C., Zheng, K., Lin, J., Yang, W. *et al.* (2006) Suppression of reactive oxygen species and neurodegeneration by the PGC-1 transcriptional coactivators. *Cell*, **127**, 397–408.

17. Weydt, P., Pineda, V.V., Torrence, A.E., Libby, R.T., Satterfield, T.F., Lazarowski, E.R., Gilbert, M.L., Morton, G.J., Bammler, T.K., Strand, A.D. *et al.* (2006) Thermoregulatory and metabolic defects in Huntington's disease transgenic mice implicate PGC-1alpha in Huntington's disease neurodegeneration. *Cell Metab.*, **4**, 349–362.

18. Cui, L., Jeong, H., Borovecki, F., Parkhurst, C.N., Tanese, N. and Krainc, D. (2006) Transcriptional repression of PGC-1alpha by mutant huntingtin leads to mitochondrial dysfunction and neurodegeneration. *Cell*, **127**, 59–69.

19. Qin, W., Haroutunian, V., Katsel, P., Cardozo, C.P., Ho, L., Buxbaum, J.D. and Pasinetti, G.M. (2009) PGC-1alpha expression decreases in the Alzheimer disease brain as a function of dementia. *Arch. Neurol.*, **66**, 352–361.

20. Zheng, B., Liao, Z., Locascio, J.J., Lesniak, K.A., Roderick, S.S., Watt, M.L., Eklund, A.C., Zhang-James, Y., Kim, P.D., Hauser, M.A. *et al.* (2010) PGC-1alpha, a potential therapeutic target for early intervention in Parkinson's disease. *Sci. Transl. Med.*, **2**, 52ra73.

21. Pacelli, C., De Rasmo, D., Signorile, A., Grattagliano, I., di Tullio, G., D'Orazio, A., Nico, B., Comi, G.P., Ronchi, D., Ferranini, E. *et al.* (2011) Mitochondrial defect and PGC-1alpha dysfunction in parkin-associated familial Parkinson's disease. *Biochim. Biophys. Acta.*, **1812**, 1041–1053.

22. Weydt, P., Soyal, S.M., Gellera, C., Didonato, S., Weidinger, C., Oberkofler, H., Landwehrmeyer, G.B. and Patsch, W. (2009) The gene coding for PGC-1alpha modifies age at onset in Huntington's Disease. *Mol. Neurodegener.*, **4**, 3.

23. Zhao, W., Varghese, M., Yemul, S., Pan, Y., Cheng, A., Marano, P., Hassan, S., Vempati, P., Chen, F., Qian, X. *et al.* (2011) Peroxisome proliferator activator receptor gamma coactivator-1alpha (PGC-1alpha) improves motor performance and survival in a mouse model of amyotrophic lateral sclerosis. *Mol. Neurodegener.*, **6**, 51.

24. Liang, H., Ward, W.F., Jang, Y.C., Bhattacharya, A., Bokov, A.F., Li, Y., Jernigan, A., Richardson, A. and Van Remmen, H. (2011) PGC-1alpha protects neurons and alters disease progression in an amyotrophic lateral sclerosis mouse model. *Muscle Nerve*, **44**, 947–956.

25. Shimizu, S., Eguchi, Y., Kamiike, W., Funahashi, Y., Mignon, A., Lacronique, V., Matsuda, H. and Tsujimoto, Y. (1998) Bcl-2 prevents apoptotic mitochondrial dysfunction by regulating proton flux. *Proc. Natl Acad. Sci. USA*, **95**, 1455–1459.

26. Cowell, R.M., Blake, K.R. and Russell, J.W. (2007) Localization of the transcriptional coactivator PGC-1alpha to GABAergic neurons during maturation of the rat brain. *J. Comp. Neurol.*, **502**, 1–18.

27. Lucas, E.K., Markwardt, S.J., Gupta, S., Meador-Woodruff, J.H., Lin, J.D., Overstreet-Wadiche, L. and Cowell, R.M. (2010) Parvalbumin deficiency and GABAergic dysfunction in mice lacking PGC-1alpha. *J. Neurosci.*, **30**, 7227–7235.

28. Azeredo da Silveira, S., Schneider, B.L., Cifuentes-Diaz, C., Sage, D., Abbas-Terki, T., Iwatsubo, T., Unser, M. and Aebischer, P. (2009) Phosphorylation does not prompt, nor prevent, the formation of alpha-synuclein toxic species in a rat model of Parkinson's disease. *Hum. Mol. Genet.*, **18**, 872–887.

29. Andreyev, A.Y., Kushnareva, Y.E. and Starkov, A.A. (2005) Mitochondrial metabolism of reactive oxygen species. *Biochemistry (Mosc.)*, **70**, 200–214.

30. Bauer, M.K., Schubert, A., Rocks, O. and Grimm, S. (1999) Adenine nucleotide translocase-1, a component of the permeability transition pore, can dominantly induce apoptosis. *J. Cell Biol.*, **147**, 1493–1502.

31. Halestrap, A.P. (2004) Mitochondrial permeability: dual role for the ADP/ATP translocator? *Nature*, **430**, 1 following 983.

32. Echtay, K.S., Roussel, D., St-Pierre, J., Jekabsons, M.B., Cadenas, S., Stuart, J.A., Harper, J.A., Roebuck, S.J., Morrison, A., Pickering, S. *et al.* (2002) Superoxide activates mitochondrial uncoupling proteins. *Nature*, **415**, 96–99.

33. Talbot, D.A., Lambert, A.J. and Brand, M.D. (2004) Production of endogenous matrix superoxide from mitochondrial complex I leads to activation of uncoupling protein 3. *FEBS Lett.*, **556**, 111–115.

34. Zhang, J. and Ney, P.A. (2009) Role of BNIP3 and NIX in cell death, autophagy, and mitophagy. *Cell Death Differ.*, **16**, 939–946.

35. Li, Y., Huang, T.T., Carlson, E.J., Melov, S., Ursell, P.C., Olson, J.L., Noble, L.J., Yoshimura, M.P., Berger, C., Chan, P.H. *et al.* (1995) Dilated cardiomyopathy and neonatal lethality in mutant mice lacking manganese superoxide dismutase. *Nat. Genet.*, **11**, 376–381.

36. Wagner, O.I., Lifshitz, J., Janmey, P.A., Linden, M., McIntosh, T.K. and Leterrier, J.F. (2003) Mechanisms of mitochondria-neurofilament interactions. *J. Neurosci.*, **23**, 9046–9058.

37. Miller, K.E. and Sheetz, M.P. (2004) Axonal mitochondrial transport and potential are correlated. *J. Cell Sci.*, **117**, 2791–2804.

38. Willy, P.J., Murray, I.R., Qian, J., Busch, B.B., Stevens, W.C. Jr, Martin, R., Mohan, R., Zhou, S., Ordentlich, P., Wei, P. *et al.* (2004) Regulation of PPARgamma coactivator 1alpha (PGC-1alpha) signaling by an estrogen-related receptor alpha (ERRalpha) ligand. *Proc. Natl Acad. Sci. USA*, **101**, 8912–8917.

39. Spina, M.B. and Cohen, G. (1989) Dopamine turnover and glutathione oxidation: implications for Parkinson disease. *Proc. Natl Acad. Sci. USA*, **86**, 1398–1400.

40. Maetzler, W., Nitsch, C., Bendfeldt, K., Racay, P., Vollenweider, F. and Schwaller, B. (2004) Ectopic parvalbumin expression in mouse forebrain neurons increases excitotoxic injury provoked by ibotenic acid injection into the striatum. *Exp. Neurol.*, **186**, 78–88.

41. Li, Z., Okamoto, K., Hayashi, Y. and Sheng, M. (2004) The importance of dendritic mitochondria in the morphogenesis and plasticity of spines and synapses. *Cell*, **119**, 873–887.

42. Kang, J.S., Tian, J.H., Pan, P.Y., Zald, P., Li, C., Deng, C. and Sheng, Z.H. (2008) Docking of axonal mitochondria by syntaphilin controls their mobility and affects short-term facilitation. *Cell*, **132**, 137–148.

43. Chang, D.T., Honick, A.S. and Reynolds, I.J. (2006) Mitochondrial trafficking to synapses in cultured primary cortical neurons. *J. Neurosci.*, **26**, 7035–7045.

44. Davey, G.P., Peuchen, S. and Clark, J.B. (1998) Energy thresholds in brain mitochondria. Potential involvement in neurodegeneration. *J. Biol. Chem.*, **21**, 12753–12757.

45. Sulzer, D. (2007) Multiple hit hypotheses for dopamine neuron loss in Parkinson's disease. *Trends Neurosci.*, **30**, 244–250.

46. Lehman, J.J., Barger, P.M., Kovacs, A., Saffitz, J.E., Medeiros, D.M. and Kelly, D.P. (2000) Peroxisome proliferator-activated receptor gamma coactivator-1 promotes cardiac mitochondrial biogenesis. *J. Clin. Invest.*, **106**, 847–856.

47. Russell, L.K., Mansfield, C.M., Lehman, J.J., Kovacs, A., Courtois, M., Saffitz, J.E., Medeiros, D.M., Valencik, M.L., McDonald, J.A. and Kelly, D.P. (2004) Cardiac-specific induction of the transcriptional coactivator peroxisome proliferator-activated receptor gamma coactivator-1alpha promotes mitochondrial biogenesis and reversible cardiomyopathy in a developmental stage-dependent manner. *Circ. Res.*, **94**, 525–533.

48. Miura, S., Tomitsuka, E., Kamei, Y., Yamazaki, T., Kai, Y., Tamura, M., Kita, K., Nishino, I. and Ezaki, O. (2006) Overexpression of peroxisome proliferator-activated receptor gamma co-activator-1alpha leads to muscle atrophy with depletion of ATP. *Am. J. Pathol.*, **169**, 1129–1139.

49. Bonen, A. (2009) PGC-1alpha-induced improvements in skeletal muscle metabolism and insulin sensitivity. *Appl. Physiol. Nutr. Metab.*, **34**, 307–314.

50. Shin, J.H., Ko, H.S., Kang, H., Lee, Y., Lee, Y.I., Pletinkova, O., Troconso, J.C., Dawson, V.L. and Dawson, T.M. (2011) PARIS (ZNF746) repression of PGC-1alpha contributes to neurodegeneration in Parkinson's disease. *Cell*, **144**, 689–702.

51. Breidert, T., Callebert, J., Heneka, M.T., Landreth, G., Launay, J.M. and Hirsch, E.C. (2002) Protective action of the peroxisome proliferator-activated receptor-gamma agonist pioglitazone in a mouse model of Parkinson's disease. *J. Neurochem.*, **82**, 615–624.

52. Swanson, C.R., Joers, V., Bondarenko, V., Brunner, K., Simmons, H.A., Ziegler, T.E., Kemnitz, J.W., Johnson, J.A. and Emborg, M.E. (2011) The PPAR-gamma agonist pioglitazone modulates inflammation and induces neuroprotection in parkinsonian monkeys. *J. Neuroinflammation*, **8**, 91.

53. Kumar, P., Kaundal, R.K., More, S. and Sharma, S.S. (2009) Beneficial effects of pioglitazone on cognitive impairment in MPTP model of Parkinson's disease. *Behav. Brain Res.*, **197**, 398–403.

54. Dusonchet, J., Bensadoun, J.C., Schneider, B.L. and Aebischer, P. (2009) Targeted overexpression of the parkin substrate Pael-R in the nigrostriatal system of adult rats to model Parkinson's disease. *Neurobiol. Dis.*, **35**, 32–41.

55. Pruszak, J., Just, L., Isacson, O. and Nikkhah, G. (2009) Isolation and culture of ventral mesencephalic precursor cells and dopaminergic neurons from rodent brains. *Curr. Protoc. Stem Cell Biol.*, Chapter 2, Unit 2D 5.

56. Livak, K.J. and Schmittgen, T.D. (2001) Analysis of relative gene expression data using real-time quantitative PCR and the 2(-Delta Delta C(T)) method. *Methods*, **25**, 402–408.

57. Schmittgen, T.D. and Livak, K.J. (2008) Analyzing real-time PCR data by the comparative C(T) method. *Nat. Protoc.*, **3**, 1101–1108.

58. Dusonchet, J., Kochubey, O., Stafa, K., Young, S.M. Jr, Zufferey, R., Moore, D.J., Schneider, B.L. and Aebischer, P. (2011) A rat model of progressive nigral neurodegeneration induced by the Parkinson's disease-associated G2019S mutation in LRRK2. *J. Neurosci.*, **31**, 907–912.